INFECTION AND IMMUNITY, May 2007, p. 2511–2522 Vol. 75, No. 5
0019-9567/07/$08.00+0 doi:10.1128/IAI.01818-06


# Primary Infection of C57BL/6 Mice with *Plasmodium yoelii* Induces a Heterogeneous Response of NKT Cells[▽]

Valérie Soulard,[1] Jacques Roland,[1] Christèle Sellier,[1] Anne Charlotte Gruner,[2,3,4] Maria Leite-de-Moraes,[5] Jean-François Franetich,[6] Laurent Rénia,[2,3,4] Pierre-André Cazenave,[1] and Sylviane Pied[1]*

*Unité d'Immunophysiopathologie Infectieuse, CNRS URA 1961, Université Paris VI, Institut Pasteur, Paris, France[1]; Département d'Immunologie, Institut Cochin, INSERM U567,[2] CNRS UMR 8104,[3] and Hôpital Cochin,[4] Université René Descartes, Paris, France; CNRS UMR 8147, Université Paris V, Hôpital Necker, Paris, France[5]; and INSERM U511, CHU La Pitié-Salpêtrière, Université Paris VI, Paris, France[6]*

Received 15 November 2006/Returned for modification 14 January 2007/Accepted 10 February 2007

**NKT cells are a population of innate-like lymphocytes that display effector functions and immunoregulatory properties. We characterized the NKT cell response induced in C57BL/6 mice during a primary infection with *Plasmodium yoelii* sporozoites. We observed a heterogeneous NKT cell response that differed between liver and spleen. Hepatic NKT cells found in infected livers consisted mainly of CD1d-dependent $CD4^+$ and double-negative (DN) NKT cells, whereas CD1d-independent NKT cells exhibiting a $TCR^{high}$ $CD4^{high}$ phenotype were prominent among splenic NKT cells during the infection. Hepatic and splenic NKT cells isolated from infected mice were activated and secreted mainly gamma interferon and tumor necrosis factor alpha in response to stimulation. Finally, *P. yoelii*-activated hepatic DN NKT cells inhibited the parasite's liver stage in a CD1d-dependent manner in vitro. However, experiments using B6.CD1d-deficient mice showed that CD1d and CD1d-restricted NKT cells are not necessary to control the parasite's development in vivo during neither the preerythrocytic stage nor the erythrocytic stage. Thus, our results show that a primary *P. yoelii* infection induces a heterogeneous and organ-specific response of NKT cells and that CD1d-dependent NKT cells play a minor role in the control of the development of *Plasmodium* in vivo in our model.**

Malaria is one of the most important parasitic diseases in humans and is a major public health problem worldwide (WHO, World Health Report 2005) (31). Mammals become infected when sporozoites are injected through their derma during the blood meal of an infected female mosquito. The sporozoites then travel to the liver through the bloodstream. Once in the liver, they invade hepatocytes, within which they differentiate into schizonts containing thousands of merozoites. This first phase of the infection is named the preerythrocytic stage. It is followed by the erythrocytic stage, which starts when merozoites, released from mature hepatic schizonts, invade red blood cells.

Infection of humans, as well as nonhuman primates or rodents, with *Plasmodium* parasites induces an immune response, which can be protective or pathogenic. The outcome of this immune response depends on several factors including the parasite strain, the host immunological history, and the host genetic background (40). Components of both the innate and the adaptive immune systems are involved in the control of *Plasmodium* development (6, 26, 46). In this context, we and others showed that the innate immune response, involving dendritic cells, NK cells, and NKT cells, can exert a direct antiparasitic activity and can also enhance the adaptive immune response to *Plasmodium* (38, 39, 47, 49).

NKT cells are innate-like lymphocytes that account for 30% to 50% of T cells in the liver, the organ where the first steps of *Plasmodium* development take place, and approximately 5% of T lymphocytes in other organs such as the spleen (2). These cells share phenotypic and functional characteristics of T and NK cells: they express a T-cell receptor αβ (TCRαβ), the CD4 or the CD8 coreceptor or neither of them (double-negative [DN] phenotype), the NK1.1 marker, and some Ly49 receptors. They also display an activated-memory phenotype (reviewed in references 11 and 21). NKT cells can be divided into three subgroups according to their TCR, antigen-presenting molecule specificity, and surface phenotype (11). The majority of NKT cells is restricted by CD1d, a nonclassical class I molecule that associates with various lipid antigens of both self-origin and foreign origin (3, 10, 53). Among these CD1d-dependent NKT cells, the "invariant NKT cells" or type I NKT cells have been the most extensively studied (11). These cells can be specifically activated by CD1d tetramers loaded with α-galactosylceramide (α-Galcer), a specific but artificial ligand (19). The second group of NKT cells is composed of CD1d-dependent type II NKT cells that can be distinguished from type I NKT cells on the basis of their TCR repertoire (11). The third group consists of CD1d-independent NKT-like cells (11).

NKT cells are involved in immune responses to tumors and to numerous infectious agents such as bacteria, viruses, and parasites (reviewed in references 3 and 15). Following activation, they rapidly produce large amounts of both Th1- and Th2-type cytokines and can also display direct cytotoxic activity (3). It was shown that CD1d-restricted NKT cells are involved in the protection as well as the pathology of *Plasmodium* infection in mice. On the one hand, CD1d-dependent NKT cells

* Corresponding author. Mailing address: Unité d'Immunophysiopathologie Infectieuse, Institut Pasteur, 25-28 rue du Docteur Roux, 75724 Paris Cedex 15, France. Phone: 00 33 1 45 68 84 65. Fax: 00 33 1 40 61 30 66. E-mail: spied@pasteur.fr.
▽ Published ahead of print on 16 February 2007.

enhance the antiplasmodial antibody response following primary infection with *Plasmodium berghei* ANKA (17). In addition, in vivo artificial activation of invariant type I NKT cells with α-Galcer inhibits *Plasmodium yoelii* 17XNL liver stage development and enhances the protective T-cell response in mice immunized with *P. berghei* NK65 or *P. yoelii* 17XNL. These effects are mediated through gamma interferon (IFN-γ) secreted by α-Galcer-activated invariant NKT cells (12). On the other hand, CD1d-dependent NKT cells are involved in the pathogenic immune response induced during *P. berghei* ANKA infection. Indeed, depending on the host genetic background, CD1d-restricted NKT cells affect the Th1/Th2 balance, pathogenesis, and fatality of murine cerebral malaria (16).

We are interested in defining the basis of a protective immune response induced during a primary *Plasmodium* infection. To this end, we studied the cellular immune response induced in naive B6 mice during an infection with *P. yoelii* 265BY initiated by the injection of sporozoites, the natural invasive form of the parasite. In this rodent model of nonlethal malaria, the mice control the infection and clear their parasitemia within 3 weeks. Our previous work showed that without exogenous stimulation, NKT cells expand in the liver of B6 mice during primary infection with *P. yoelii* 265BY sporozoites (34). These cells inhibited the parasite's growth within hepatocytes in vitro, and our data suggested that DN NKT cells are the main actors in this antiparasitic activity, partially mediated by IFN-γ (34).

The aim of the present work was to better characterize the NKT cell response induced during a primary *P. yoelii* 265BY infection in B6 mice and to evaluate its contribution to the control of parasite development further. We observed a heterogeneous NKT cell response that differed between liver and spleen. Different subpopulations of $CD4^+$ and DN NKT cells, comprising CD1d-dependent and -independent cells and invariant and noninvariant cells, were elicited in these organs during the infection. Interestingly, in the spleens of *P. yoelii*-infected mice, we observed the appearance of a population of CD1d-independent NKT cells exhibiting an unusual $TCR^{high}$ $CD4^{high}$ phenotype. Both hepatic and splenic NKT cells were activated and secreted mainly IFN-γ and tumor necrosis factor alpha (TNF-α) following short-term stimulation in vitro. We also found that *P. yoelii*-activated hepatic DN NKT cells inhibited the growth of the parasite within hepatocytes in a CD1d-dependent manner in vitro. However, B6.CD1d-deficient and B6 control mice exhibited the same amount of parasite within their livers and the same parasitemia following infection. These results show that during a primary infection, CD1d and CD1d-dependent NKT cells are not necessary to limit the development of *P. yoelii* in vivo during neither the preerythrocytic stage nor the erythrocytic stage.

## MATERIALS AND METHODS

**Mice.** C57BL/6N@Ico mice were purchased from Charles River-Iffa Credo (L'Arbresle, France). CD1d.1$^{-/-}$ mice on a C57BL/6 genetic background were provided by A. Bendelac (5). All animals were bred and housed in the animal facilities of the Department of Immunology at the Institut Pasteur (Paris, France) under standard conditions. Only 8- to 12-week-old females were used for the experiments, which were conducted in accordance with institutional guidelines for animal care and use.

**Parasites, in vivo infection, and parasitemia.** *P. yoelii yoelii* (nonlethal strain 265BY) sporozoites were obtained by dissecting the salivary glands of infected *Anopheles stephensi* mosquitoes as previously described (28). The mosquitoes were bred, maintained, and infected at the INSERM U511 insectarium (La Pitié-Salpêtrière, Paris, France) and the Centre de Production et Infection des Anophèles, Institut Pasteur, Paris, France. Mice were infected intravenously with 4,000 sporozoites diluted in sterile phosphate-buffered saline (PBS). Parasitemia was measured on Giemsa-stained thin blood smears. Results are expressed as the percentage of parasitized erythrocytes (RBCs).

**Isolation of hepatic and splenic mononuclear cells.** Hepatic mononuclear cells were prepared as previously described (51). Briefly, livers from control and infected mice were perfused in situ with sterile Dulbecco's modified Eagle's medium (DMEM), removed, and homogenized using a Potter-Elvehjem homogenizer. Cells were washed, resuspended in a 35% Percoll solution (Pharmacia Biotech, Uppsala, Sweden), and centrifuged at 1,400 × *g* for 25 min at room temperature (RT). The pellet (containing mononuclear cells) was washed with DMEM. Spleens from control and infected mice were gently smashed between two glass slides in DMEM and washed in DMEM. Hepatic and splenic cell suspensions were then treated with an ACK lysing buffer (0.15 M $NH_4Cl$, 10 mM $KHCO_3$, 0.1 mM $Na_2EDTA$) to lyse RBCs. Finally, hepatic and splenic cells were resuspended in PBS containing 3% fetal calf serum (FCS) before counting and staining for flow cytometry analysis.

**Flow cytometry analysis.** Liver and splenic cells from control and infected mice were stained at 4°C in PBS supplemented with 3% FCS using the following monoclonal antibodies (mAbs) purchased from BD Pharmingen, unless otherwise specified, conjugated to fluorescein isothiocyanate (FITC), phycoerythrin (PE), peridinin chlorophyll protein, allophycocyanin (APC), or biotin: anti-TCRβ (H57-597), anti-CD3 ε (145-2C11), anti-NK1.1 (PK136), anti-CD4 (H129.19), anti-CD8α (53-6.7), anti-CD69 (H1.2F3), anti-CD62L (Mel-14), anti-Ly49C/I (SW5E6), anti-Ly49G2 (4D11), anti-Ly49D (4E5), and anti-Ly49A (JR9-318) (37). Quantum red-conjugated streptavidin (Tebu-bio, Le Perray en Yvelines, France), PE–cyanin-7-conjugated streptavidin (BD Pharmingen), or APC-conjugated streptavidin (BD Pharmingen) was used to reveal biotin-coupled mAb.

Vα14-Jα18 invariant NKT cells were stained under the same conditions using APC-conjugated CD1d tetramers loaded with α-Galcer and empty APC-conjugated CD1d tetramers as a control (43). Cells were incubated with Fc Block (2.4G2; BD Pharmingen) prior to incubation with the tetramers.

When possible, dead cells were excluded by propidium iodide (Sigma-Aldrich, Saint Quentin Fallavier, France) staining. Stained cells were analyzed on a four-color FACSCalibur flow cytometer using CellQuest 3.3 software or a six-color LSR flow cytometer with CellQuest Pro software (BD Biosciences, San Diego, CA).

**Purification of hepatic DN NKT cells for in vitro functional assays.** Hepatic mononuclear cells were isolated from a pool of livers removed from B6 mice 10 days after infection with 4,000 sporozoites. Cells were incubated with PE-conjugated anti-CD8α and anti-CD19 (1.D3; BD Pharmingen) mAbs. Stained cells were washed in a solution containing PBS, 0.5% FCS, and 2.5 mM EDTA and incubated in this buffer with anti-PE-coated magnetic microbeads (Miltenyi Biotec, Bergisch-Gladbach, Germany). CD8α- and CD19-positive cells were depleted on an automated magnetic cell sorter (AutoMACS; Miltenyi Biotec) using the Depletes program. Prior to staining for the cell sorting, the depletion was checked on a flow cytometer. Cells were then incubated with FITC-conjugated anti-CD5 mAb (53-7.3; BD Pharmingen), PE-conjugated anti-NK1.1 mAb, and biotin-conjugated anti-CD4, which was revealed with PE–cyanin-7-conjugated streptavidin.

$NK1.1^+$ $CD5^+$ DN ($CD4^-$ $CD8^-$) cells were sorted by flow cytometry using a MoFlo cell sorter (Cytomation, Inc., Ft. Collins, CO). Cell purity was between 94% and 99%. Finally, cells were counted (viability, as estimated by eosin incorporation, was >99%), washed, and resuspended in complete William's medium E (Life Technologies, Edinburgh, Scotland) before adding them to primary infected hepatocyte cultures.

**Primary culture of hepatocytes and in vitro infection with *P. yoelii*.** Hepatocytes from B6 or B6.CD1d$^{-/-}$ mice were prepared as previously described (35). Briefly, a hepatic lobe was removed and perfused with HEPES buffer and a collagenase solution {1.2 *N*-(3-[2-furyl]acryloyl)-Leu-Gly-Pro-Ala (FALGPA) units/ml, collagenase type IV; Sigma Aldrich Chemie Gmbh, Schnelldorf, Germany}. Cells were washed once in complete William's medium E containing 10% FCS (Eurobio, Courtaboeuf, France), 2 mM glutamine (GibcoBRL, Life Technologies, Cergy Pontoise, France), and 100 IU/ml penicillin-streptomycin (GibcoBRL) and then overlaid on a 60% Percoll solution (Pharmacia Biotech, Uppsala, Sweden). Hepatocytes were recovered by centrifugation (800 × *g*) at RT for 3 min. The pellet was washed once in complete William's medium E. Cell viability was assayed by eosin staining (>90%), and purity was estimated by cell morphology (>95%). Hepatocytes were then distributed into eight-well plastic

Lab Tek slides (Nunc, Naperville, IL) at a concentration of $8 \times 10^4$ cells per well. Wells had been precoated with collagen to optimize cell adhesion and viability (collagen type I from rat tail; Sigma-Aldrich). After 24 h at 37°C in a 3.5% $CO_2$ atmosphere, the medium was removed, and $1.5 \times 10^5$ sporozoites per well were added in 150 μl of complete William's medium E supplemented with 10 μg/ml gentamicin (Sigma-Aldrich). Three hours later, medium was replaced with fresh complete William's medium E.

**In vitro assay of *P. yoelii* liver-stage development inhibition by parasite-activated hepatic DN NKT cells.** Three hours after infecting cultured hepatocytes with sporozoites, sorted NK1.1$^+$ CD5$^+$ DN cells from infected animals were added to the culture wells at different ratios to test their capacity to inhibit the liver-stage development of the parasite. Forty-five hours later, infected hepatocyte cultures were fixed in cold methanol. Cells were then incubated for 1 h at RT with an immune serum specific for the *P. yoelii* hepatic stage diluted in PBS, washed, and subsequently incubated for 1 h at RT, in the dark, with a goat anti-mouse immunoglobulin G (heavy plus light chains) coupled to FITC (Caltag Laboratories, Burlingame, CA) diluted in PBS. Finally, cells were washed in PBS and mounted in Vectashield mounting medium (Vector Laboratories, Inc. Burlingame, CA). Slides were examined by fluorescence microscopy, and the numbers of intrahepatocytic parasites in control and experimental culture wells (which contained sorted cells) were determined. Schizont sizes were calculated by taking pictures of 50 schizonts, chosen at random, per well at the same magnification and measuring their diameters. Results are expressed in arbitrary units as the means of diameters ± standard deviations (SD) of the parasites in control and experimental wells. Statistical analysis was performed using the nonparametric Mann-Whitney test.

**Quantification of parasite load in the liver of C57BL/6 and B6.CD1d$^{-/-}$ mice.** Liver parasites were quantified as described previously by Hulier et al., with minor changes (18). Mice were injected intravenously with 40,000 *P. yoelii* 265BY sporozoites. Forty-four hours later, a liver biopsy was taken, frozen in liquid nitrogen, and crushed in 2 ml of digestion buffer before incubation overnight at 37°C with proteinase K (0.1 mg/ml; GibcoBRL). DNA was prepared using a classical phenol-chloroform extraction protocol. DNA was quantified by densitometry (optical density at 260 nm), and the solution was adjusted to 0.5 mg/ml with water and was then used as a template for PCR. The suitability of the purified DNA was assessed by performing PCR with primers amplifying the mouse β-actin gene. The reaction mixture contained 400 nM primers (BA-F [5′-ATGGATGACGATATCGCT-3′] and BA-R [5′-ATGAGGTAGTCTGTC AGGT-3′]), 1.5 mM $MgCl_2$, 250 μM deoxynucleoside triphosphates, 0.6 U of *Taq* polymerase (Applied Biosystems), and 0.5 μg of DNA in a total volume of 30 μl. The cycling conditions were as follows: a denaturation step at 95°C for 3 min followed by 30 cycles of 30 s of hybridization at 55°C, 1 min of elongation at 72°C, and 30 s of denaturation at 95°C. One microgram of each sample was then used as a template for real-time semiquantitative PCR using the LightCycler FastStart DNA Master SYBR green I kit (Roche, Germany) in a LightCycler apparatus (Roche, Germany). Each reaction was performed in duplicate. The primers used were NYU-Py3 (forward) (5′-GGGGATTGGTTTTGACGTTTT TGCG-3′) and NYU-Py5 (reverse) (5′-AAGCATTAAATAAAGCGAATACA TCCTTAT-3′) (4), which target the small-subunit rRNA (ssrRNA) gene of the parasite. PCR conditions were as follows: SYBR green mix was prepared as indicated by the manufacturer, with final concentrations of 3 mM $MgCl_2$ and 400 nM primers (forward and reverse) in a total volume of 20 μl. The amplification program was as follows: 95°C for 10 min followed by 40 cycles of 95°C for 10 s, 60°C for 10 s, and 72°C for 10 s. A melting curve was generated by a linear increase of temperature from 52 to 95°C at 0.2°C/s. Standard curves were generated using a series of 10-fold dilutions (from $10^6$ to 10 parasite nuclei/μl) of DNA solution purified from blood stages of *P. yoelii*. The number of parasite nuclei/μl in this sample was determined by microscopic examination of Giemsa-stained blood smears and calculation of the number of RBCs/μl of blood. Genomic DNA was used rather than a plasmid bearing an ssrRNA gene to generate the standard curve because it reflects the multiple targets amplified more accurately, because there are more than five different ssrRNA genes in the genome of *P. yoelii*. Results are expressed as the log numbers of the parasite nuclei/0.5 μg of liver DNA. The reaction was linear down to 10 nuclei (slope of linear regression, −3.495).

**Intracellular cytokine staining.** Hepatic and splenic cells from control and infected mice were isolated and incubated at a concentration of $1 \times 10^6$ cells per ml for 3 h at 37°C in a 7% $CO_2$ atmosphere in complete RPMI medium (GibcoBRL) containing phorbol myristate A (50 ng/ml; Sigma-Aldrich), ionomycin (500 ng/ml; Sigma-Aldrich), and brefeldin A (10 μg/ml; Sigma-Aldrich). Surface antigens were then stained at 4°C in the dark for 30 min with FITC-conjugated anti-TCRβ, PE-conjugated anti-NK1.1, and peridinin chlorophyll protein-conjugated anti-CD4 and/or anti-CD8α mAbs. Cells were fixed for 1 h at RT, in the dark, with 2% paraformaldehyde and then treated with Perm/Wash solution (BD Biosciences) before incubation with APC-conjugated anti-interleukin-4 (IL-4) (11B11; BD Pharmingen), anti-IFN-γ (XMG1.2; BD Pharmingen), or anti-TNF-α (MP6-XT22; BD Pharmingen) mAb in Perm/Wash solution at RT, in the dark, for 30 min. Finally, cells were washed in Perm/Wash solution and then washed in PBS containing 1% bovine serum albumin and resuspended in PBS containing 3% FCS. Staining was analyzed on a FACSCalibur flow cytometer using Cell Quest 3.3 software (BD Biosciences). Gates were done on CD4$^+$ CD8$^+$ cells and CD4$^-$ CD8$^-$ (DN) cells. CD4$^+$ CD8$^+$ cells were considered to be representative of CD4$^+$ NKT cells, as CD8$^+$ NKT cells were a minor population among total NKT cells in infected livers. Nonstimulated splenic cells (incubated under the same conditions but without phorbol myristate acetate, ionomycin, and brefeldin A) from the same mice were stained following the same protocol and used as controls.

**Statistical analyses.** Statistical analyses were performed using the nonparametric Mann-Whitney test and Statview 5.0 software (SAS Institute Inc., Cary, NC); *P* values are indicated in the figure legends.

## RESULTS

**Phenotype of hepatic NKT cells during primary *P. yoelii* infection.** We carried out flow cytometry analysis of hepatic NKT cells from naive and infected B6 mice at different time points following the injection of sporozoites. In accordance with our previous results (34), we observed that the total number of hepatic NKT cells increased over time (Fig. 1A). We found that the number of CD4$^+$ NKT cells increased by 1.9-fold between day 0 and day 10 (Fig. 1A), even though their proportion among hepatic NKT cells decreased over time (from 79.5% ± 0.7% on day 0 to 53.3% ± 6.6% on day 10) (data not shown). The DN subpopulation tripled in size (Fig. 1A) and represented 20.1% ± 3.6% of the total NKT cells in the liver on day 10, compared to 17.7% ± 0.98% on day 0 (data not shown).

We then looked for a correlation between the increase in the numbers of NKT cells and their activation status by flow cytometry analysis of the surface expression of the CD69, CD62, and CD44 markers. All hepatic NKT cells from naive mice already displayed an activated-memory phenotype (Fig. 1B) (8), and the percentages of CD69$^+$, CD44$^{high}$, and CD62L$^-$ cells among total NKT cells did not significantly change during infection (data not shown). Nevertheless, the level of surface expression of CD69 on CD4$^+$ cells and DN hepatic NKT cells increased over time, peaking on day 6 postinfection (p.i.) (Fig. 1B). Indeed, the proportion of cells displaying a CD69$^{high}$ phenotype was considerably increased on day 6 p.i. compared to day 0 among both CD4$^+$ and DN NKT cells (reaching 73% ± 5% and 58% ± 7%, respectively) (Fig. 1C). The proportion of CD69$^{high}$ CD4$^+$ cells did not change between day 6 and day 10 p.i., while the proportion of CD69$^{high}$ DN cells declined (Fig. 1C). In addition, we detected a population of CD62L$^+$ DN NKT cells on day 6 p.i. (28.38% ± 8.35% of DN NKT cells), which was still present at day 10 p.i. (representing 46.95% ± 1.36% of DN NKT cells) (Fig. 1B). Conversely, CD4$^+$ hepatic NKT cells remained CD62L$^-$ at all time points (Fig. 1B). Finally, the level of expression of CD44 varied during the course of infection but to a lesser extent than that of the other surface markers examined (Fig. 1B).

Thus, we observed that the numbers of CD4$^+$ and DN NKT cells increased in the livers of B6 mice following injection of *P. yoelii* sporozoites and that both NKT cell subsets were activated. Interestingly, the DN subset exhibited a transient activation, as shown by the peak in the percentage of CD69$^{high}$ DN

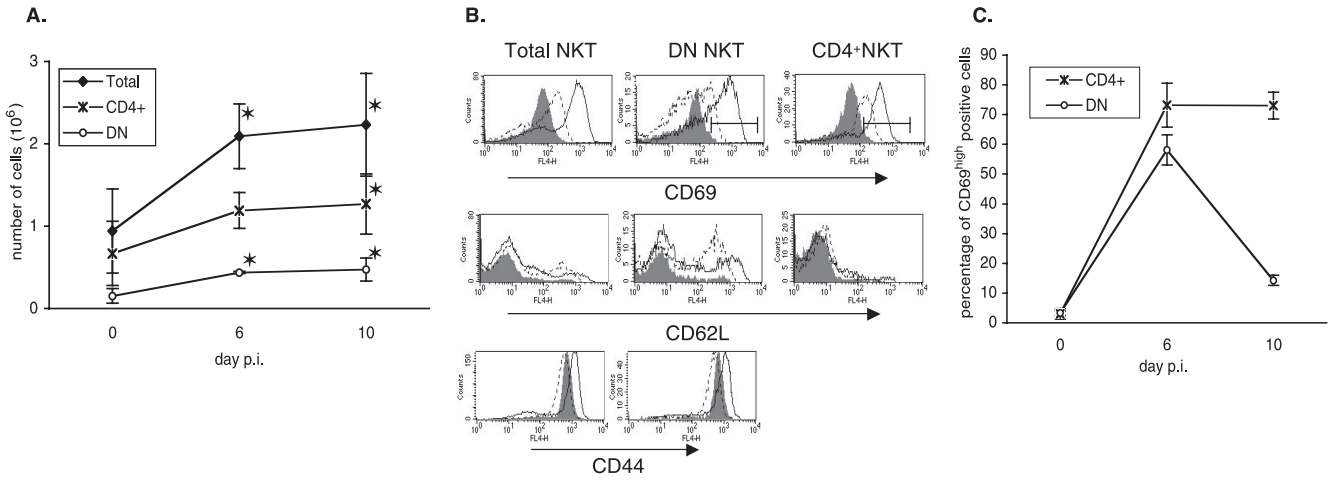


FIG. 1. Kinetic and surface phenotype of hepatic NKT cells during primary *P. yoelii* infection in C57BL/6 mice. (A) Numbers of total, $CD4^+$, and DN NKT cells in the livers of B6 mice on day 0 (noninfected) and days 6 and 10 after injection of 4,000 sporozoites. Hepatic cells were stained with anti-NK1.1, -TCRβ, -CD4, or -$CD4^+$ CD8 mAbs, and the numbers of total ($NK1.1^+$ $TCR\beta^+$), DN ($CD4^-$ $CD8^-$ $NK1.1^+$ $TCR\beta^+$), and $CD4^+$ ($CD4^+$ $NK1.1^+$ $TCR\beta^+$) NKT cells were determined by flow cytometry analysis. Data are representative of three different experiments with at least three mice per time point. Results are expressed as mean values ± SD. (B) Markers expressed by hepatic NKT cells in noninfected mice (day 0, filled histogram) and infected mice at day 6 (thin line) and day 10 (dotted line) after injection of 4,000 sporozoites. Hepatic cells were stained with anti-NK1.1, -TCRβ, -CD4, or -$CD4^+$ CD8 mAbs and anti-CD69, -CD62L, or -CD44 mAbs. Histograms are gated on total, DN, and $CD4^+$ NKT cells as defined in A. Data are representative of two independent experiments with three mice per time point. (C) Percentages of $CD69^{high}$ cells among $CD4^+$ and DN NKT cells (gates were down as shown in panel B). This is a different representation of the results shown in B, and results are expressed as mean values ± SD. ∗, the *P* value was <0.05 between control (day 0) and infected animals.

NKT cells at day 6 p.i. compared to $CD4^+$ NKT cells. We also noticed that a population of $CD62L^+$ DN NKT cells arose in the livers of infected mice.

**Phenotype of splenic NKT cells during primary *P. yoelii* infection.** Concomitantly, by using flow cytometry, we analyzed the dynamic and phenotype of splenic NKT cells from naive and infected B6 mice at different time points following sporozoite injection.

In the spleen, the number of splenic NKT cells also increased during the infection (Fig. 2A), but their percentage did not vary significantly among the total lymphoid splenic population between naive and infected mice (data not shown). This

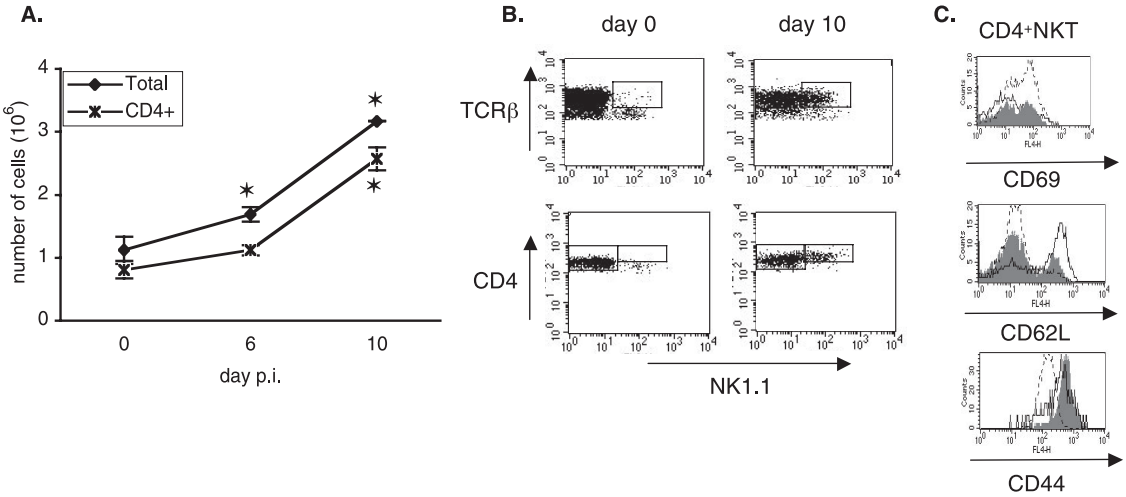


FIG. 2. Kinetic and surface phenotype of splenic NKT cells during primary *P. yoelii* infection in C57BL/6 mice. (A) Numbers of total and $CD4^+$ NKT cells in the spleens of B6 mice on day 0 (noninfected) and at days 6 and 10 after injection of 4,000 sporozoites. Splenic cells were stained with anti-NK1.1, anti-TCRβ, and anti-CD4 mAbs, and the numbers of total ($NK1.1^+$ $TCR\beta^+$) and $CD4^+$ ($NK1.1^+$ $TCR\beta^+$ $CD4^+$) NKT cells were determined by flow cytometry analysis. Data are representative of three independent experiments with at least three mice per time point. Results are expressed as mean values ± SD. (B) Flow cytometry analysis showing the level of surface expression of TCRβ and CD4 molecules on splenic $CD4^+$ NKT cells (gate was done on $NK1.1^+$ $TCR\beta^+$ $CD4^+$ cells). Representative dot plots of data from infected mice on day 0 and day 10 are shown. (C) Markers expressed by splenic NKT cells in noninfected mice (day 0, filled histogram) and infected mice at day 6 (thin line) and day 10 (dotted line) after injection of 4,000 sporozoites. Splenic cells were stained with anti-NK1.1, -TCRβ, or -CD4 and anti-CD69, -CD62L, or -CD44 mAbs. Histograms are gated on $CD4^+$ NKT cells as defined in A. Data are representative of two independent experiments with three mice per time point. ∗, the *P* value was <0.05 between control (day 0) and infected animals.

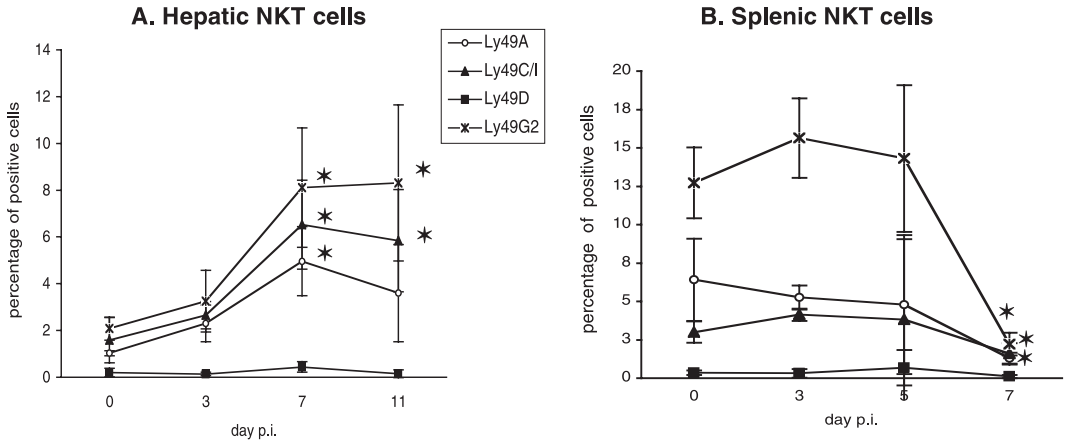


FIG. 3. Kinetics of hepatic and splenic Ly49$^+$ NKT cells during primary *P. yoelii* infection in C57BL/6 mice. Percentages of Ly49$^+$ cells among hepatic (A) and splenic (B) NKT cells in noninfected (day 0) B6 mice and at different time points after injection of 4,000 sporozoites are shown. Cells were stained with anti-NK1.1 and anti-CD3 mAbs and anti-Ly49A, -Ly49C/I, -Ly49D, or -Ly49G2 mAbs. The percentages of Ly49$^+$ cells were determined by flow cytometry analysis. Data are representative of three different experiments with three mice per time point. Results are expressed as mean values ± SD. *, the *P* value was <0.05 between control (day 0) and infected animals.

increase in the splenic NKT cells number started after day 3 of infection, and this population tripled in size between day 0 and day 10 p.i. (Fig. 2A). Most of these cells expressed the CD4 coreceptor on their surface (Fig. 2A). Indeed, CD4$^+$ cells accounted for 72.6% ± 4.8%, 66.05% ± 5.33%, and 79.07% ± 6.33% of splenic NKT cells on days 0, 6, and 10 p.i., respectively (data not shown). We therefore restricted our study in the spleen to CD4$^+$ NKT cells. It is also interesting to note that NK1.1$^+$ cells accounted for about 5% of all splenic CD4$^+$ T cells in naive mice and until day 6 p.i., but this percentage then increased, reaching 35% on day 10 p.i. (data not shown). Moreover, we observed that all the NK1.1$^+$ CD4$^+$ T cells found in the spleens of infected mice on day 10 expressed a large number of TCRs and CD4 coreceptors on their surface, as shown by their TCRβ$^{high}$ CD4$^{high}$ phenotype (Fig. 2B). The proportion of CD69$^+$ cells among the splenic CD4$^+$ NKT cells did not change significantly during infection (data not shown). However, a transient increase in the proportion of CD62L$^+$ cells occurred at day 6 p.i. (Fig. 2C) (CD62L$^+$ cells represented 52.8% ± 9.5% of the CD4$^+$ NKT cells compared to 17% ± 4% in control mice). Finally, the proportion of CD44$^+$ cells did not change during the infection, even though we noticed that the CD4$^{high}$ NKT cells became CD44$^{int}$ since day 10 p.i. (Fig. 2C).

Thus, a primary *P. yoelii* infection elicits a peculiar population of CD4$^{high}$ NKT cells in the spleens of B6 mice. These cells did not present the surface phenotype of classical NKT cells characterized by intermediate levels of TCR and NK1.1 expression on their surface (11). Furthermore, they accounted for a nonnegligible proportion of the CD4$^+$ T cells found in the spleens of B6 mice at day 10 p.i. On day 10 p.i., about 40% of the CD4$^{high}$ NKT cells found in the spleens of B6 mice expressed the activation marker CD69, and 80% did not express the adhesion molecule CD62L.

**Analysis of the Ly49 repertoire expressed by hepatic and splenic NKT cells during primary *P. yoelii* infection.** As some Ly49 receptors on NKT cells have been described and shown to play a role in the tuning of their activation throughout their development and function (25, 44, 50), we used flow cytometry to analyze the surface expression of the Ly49A, Ly49C/I, and Ly49G2 inhibitory receptors and the Ly49D activatory receptor on total hepatic and splenic NKT cells during infection. Very few NKT cells isolated from the livers of naive mice expressed Ly49 receptors (Fig. 3A) (8). Following infection with sporozoites, the proportions of Ly49A$^+$, Ly49C/I$^+$, and Ly49G2$^+$ hepatic NKT cells increased significantly in a coordinated fashion (Fig. 3A). Concerning the splenic NKT cells, we observed that the percentages of Ly49$^+$ NKT cell subpopulations remained constant until day 5 p.i. and then dramatically dropped, leading to the almost complete disappearance of these cells in the spleen at day 7 p.i. (Fig. 3B). We confirmed that NKT cells from naive B6 mice do not express the activating receptor Ly49D (44), and we observed that they do not start to express it during *P. yoelii* infection (Fig. 3A and B).

Thus, the proportion of NKT cells expressing Ly49 inhibitory receptors increases in the liver during infection and, on the contrary, decreases in the spleen. Hence, regarding the expression of these NK receptors and their peculiar TCR$^{high}$ CD4$^{high}$ phenotype, splenic NKT cells induced by the infection display a phenotype that is markedly different from that of CD4$^+$ NKT cells found in the spleens of naive mice.

**Analysis of the CD1d specificity and the TCRαβ repertoire of hepatic and splenic NKT cells elicited during primary *P. yoelii* infection.** NKT cells can be divided into different subsets according to their specificities for CD1d, a nonclassical class I molecule (8, 21). To assess the CD1d dependency of the studied subpopulations of NKT cells, we infected B6 mice and B6.CD1d-deficient mice in which only CD1d-independent NKT cells develop. We observed that the number of CD4$^+$ NKT cells in the livers of control and infected B6.CD1d-deficient mice had dramatically decreased compared to that found in the livers of infected B6 mice (Fig. 4A). The number of DN NKT cells increased in the livers of B6.CD1d-deficient mice after infection but to a lesser extent than in B6 control mice (Fig. 4B). As shown on Fig. 4C, we observed an expansion of CD4$^+$ NK1.1$^+$ T cells in the spleens of infected B6.CD1d-

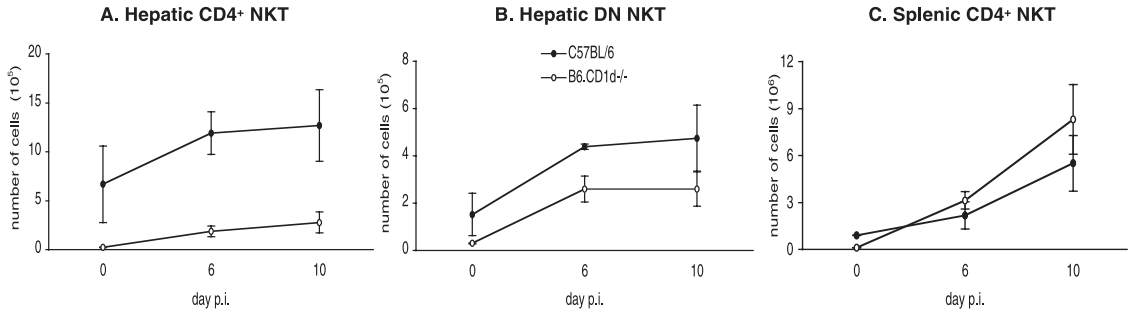


FIG. 4. Kinetics of hepatic and splenic NKT cell subpopulations during primary *P. yoelii* infection in C57BL/6 and B6.CD1d$^{-/-}$ mice. Numbers of (A) hepatic CD4$^+$ NKT cells, (B) hepatic DN NKT cells, and (C) splenic CD4$^+$ NKT cells in noninfected (day 0) B6 and B6.CD1d$^{-/-}$ mice and at days 6 and 10 postinjection (p) of 4,000 sporozoites are shown. Cells were stained with anti-NK1.1, -TCRβ, -CD4, or -CD4$^+$ CD8 mAbs, and the numbers of total (NK1.1$^+$ TCRβ$^+$), DN (CD4$^-$ CD8$^-$ NK1.1$^+$ TCRβ$^+$), and/or CD4$^+$ (CD4$^+$ NK1.1$^+$ TCRβ$^+$) NKT cells were determined by flow cytometry analysis. Data are representative of two independent experiments with four mice per time point. Results are expressed as mean values ± SD.

deficient mice comparable to that observed in wild-type B6 mice. These cells also displayed the particular CD4$^{high}$ TCR$^{high}$ phenotype that we observed for splenic NKT cells in infected spleens of B6 mice (data not shown).

These results suggest that most of the CD4$^+$ NKT cells elicited in the livers of B6 mice during infection are CD1d dependent and that the DN NKT cells present in the liver of infected B6 mice are expected to comprise both CD1d-dependent and CD1d-independent cells. On the contrary, these results suggest that splenic CD4$^{high}$ NKT cells identified in infected B6 mice are CD1d-independent NKT cells.

CD1d-dependent and -independent NKT cells express different TCRαβ repertoires (11). There are two types of CD1d-dependent NKT cells: type I invariant NKT cells, which express the TCRVα14-Jα18 chain paired with the TCRVβ8.2, Vβ7, or Vβ2 segments, and type II NKT cells, which express the TCRVα3.2 or Vα8 chains associated with the TCRVβ8 chain (11). To determine to which subset the NKT cells present within infected livers and spleens belonged, we performed flow cytometry analysis on cells from control and infected B6 mice incubated with APC-conjugated CD1d tetramers loaded with α-Galcer. These tetramers specifically stain the type I NKT cells. Empty CD1d tetramers were used as a control (Fig. 5A). Most of the CD4$^+$ NKT cells (69.2% ± 1.9%) present in infected livers on day 10 were stained with CD1d tetramers loaded with α-Galcer, showing that these cells

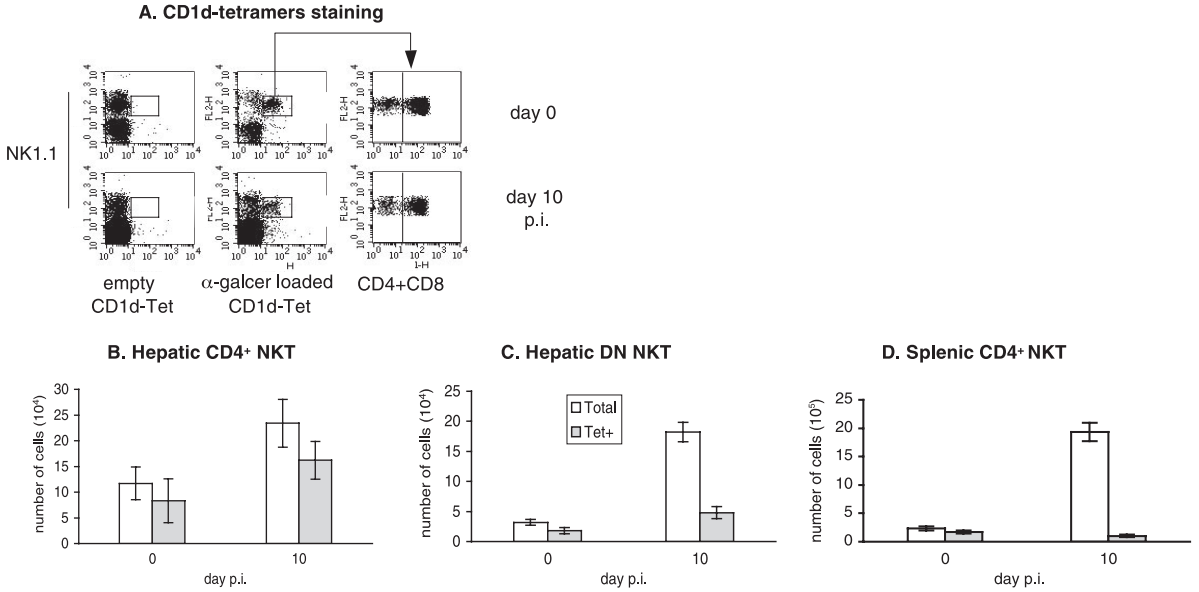


FIG. 5. Numbers of hepatic and splenic invariant NKT cells in C57BL/6 mice during primary *P. yoelii* infection. Cells were stained with anti-NK1.1, -TCRβ, -CD4, or -CD4$^+$ CD8 mAbs and CD1d tetramers (Tet) loaded with α-Galcer (α-galcer loaded CD1d Tet). Empty tetramers were used as controls. (A) Representative flow cytometry analysis of hepatic DN NKT cells (gated on TCRβ$^+$ cells). (B) Numbers of total (CD4$^+$ NK1.1$^+$ TCRβ$^+$) and Tet$^+$ (α-Galcer-loaded CD1d Tet$^+$ CD4$^+$ NK1.1$^+$ TCRβ$^+$) CD4$^+$ hepatic NKT cells as determined by flow cytometry analysis. (C) Numbers of total (CD4$^-$ CD8$^-$ NK1.1$^+$ TCRβ$^+$) and Tet$^+$ (α-Galcer CD1d Tet$^+$ CD4$^-$ CD8$^-$ NK1.1$^+$ TCRβ$^+$) DN hepatic NKT cells. (D) Numbers of total (CD4$^+$ NK1.1$^+$ TCRβ$^+$) and Tet$^+$ (α-Galcer-loaded CD1d Tet$^+$ CD4$^+$ NK1.1$^+$ TCRβ$^+$) CD4$^+$ splenic NKT cells. Data are representative of two independent experiments performed with at least three mice per group. Results are expressed as mean values ± SD.

belong to the type I population of NKT cells (Fig. 5B). On the contrary, the hepatic DN NKT cells were mostly noninvariant NKT cells, as only 26.19% ± 4.08% of these cells were stained with the tetramers at day 10 p.i. (numbers of cells are shown in Fig. 5C). These results are consistent with those for infected B6.CD1d-deficient mice (Fig. 4A and B). As shown in Fig. 5D, most of the NKT cells found in infected spleens were not stained with the tetramers (on days 0 and 10 p.i., $CD4^{high}$ NKT cells stained with tetramers [$CD4^{high}$ NKT $Tet^+$ cells] accounted for about 73% and 5%, respectively, of total $CD4^{high}$ NKT cells). These results are also consistent with those obtained for infected B6.CD1d-deficient mice (Fig. 4C) and show that the majority of the $CD4^{high}$ NKT cells found in spleens of infected B6 mice are not invariant NKT cells.

We further analyzed the TCRVβ repertoire of the subpopulations of NKT cells during infection. We used flow cytometry to examine Vβ8 and Vβ7 chain usage by NKT cells. In the livers of naive B6 mice, 75.8% of $CD4^+$ and 63.5% of DN NKT cells were $V\beta8.1^+$, $V\beta8.2^+$, or $V\beta7^+$; these proportions did not change significantly during infection (data not shown). These results reinforce the idea that the $CD4^+$ NKT cells present in the liver until day 10 p.i. are mainly type I CD1d-dependent NKT cells expressing the TCRVα14-Jα18 invariant chain associated with TCRVβ8 or Vβ7 segments. On the other hand, the DN NKT cells elicited in the livers of B6 mice during infection consist of type I and type II CD1d-dependent NKT cells in addition to CD1d-independent NKT cells. Indeed, the presence of TCRVβ8- and Vβ7-negative cells among the DN NKT cell population confirms that around 40% of these cells are CD1d-independent NKT cells, which presumably belong to the type III NKT-like subset expressing a diverse TCRαβ repertoire (11).

We found that only 10 to 15% of the $CD4^{high}$ NKT cells present in the spleens of B6 mice at day 10 of infection expressed the Vβ8.1/Vβ8.2 and Vβ7 chains of the TCR, whereas these chains were expressed by 60% of splenic $CD4^+$ NKT cells present in naive mice (data not shown). The peculiar population of $CD4^{high}$ NKT cells found in the spleens of infected B6 mice can therefore be considered to consist predominantly of noninvariant, CD1d-independent cells presenting no bias in the expression of the Vβ8 and Vβ7 chains of the TCR. Overall, these results suggest that these cells are type III NKT cells (11).

**Profiles of cytokines produced by *P. yoelii*-activated hepatic and splenic NKT cells in response to in vitro stimulation.** To obtain insight into the function of the NKT cells during primary infection, we used flow cytometry to analyze the cytokines produced by these cells isolated from the livers and spleens of naive and infected B6 mice. For this purpose, hepatic and splenic cells were isolated and stimulated in vitro prior to intracellular staining of cytokines and fluorescence-activated cell sorter analysis.

Under these conditions, 55% and 75% of the total hepatic NKT cells recovered from mice on days 5 and 7 p.i., respectively, produced TNF-α and IFN-γ, whereas only 6% and 20% produced IL-4 (data not shown). At day 10 p.i., the number of hepatic $CD4^+$ NKT cells producing TNF-α, IFN-γ, and IL-4 increased, and this population represented the major source of these cytokines among hepatic NKT cells (Fig. 6A). The number of hepatic DN NKT cells producing TNF-α and IFN-γ started to increase after day 5 p.i. (Fig. 6B). At this time point, the DN subset represented, in numbers of cells, the main source of IFN-γ among hepatic total NKT cells. Interestingly, we observed a marked difference between the two subsets of hepatic NKT cells: $CD4^+$ NKT cells produced both IFN-γ and TNF-α and IL-4 cytokines (Fig. 6A), whereas DN NKT cells displayed a bias towards the production of IFN-γ and TNF-α (Fig. 6B). We also observed that the increase in the numbers of IFN-γ- and TNF-α-producing DN NKT cells correlates with the peak in the proportion of $CD69^{high}$ cells among this population (Fig. 1C). As shown in Fig. 6C, the $CD4^+$ NKT cells present in the spleens of infected mice were also biased towards the capacity to produce TNF-α and IFN-γ but not IL-4.

Thus, our results show that the numbers of hepatic NKT cells producing TNF-α, IFN-γ, and IL-4 in response to stimu-

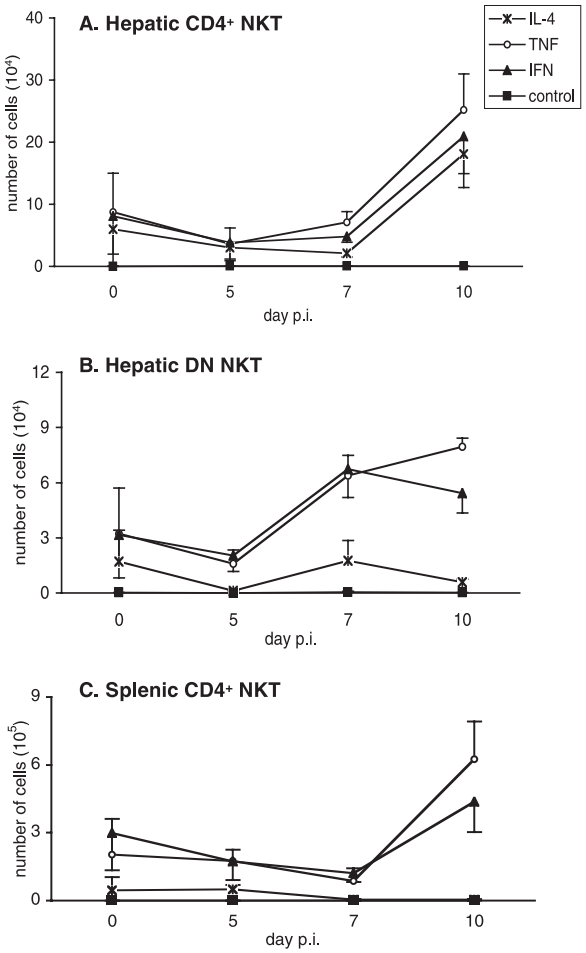


FIG. 6. Cytokine profile of hepatic and splenic NKT cells during primary *P. yoelii* infection in C57BL/6 mice. The production of IL-4, TNF-α, and IFN-γ by hepatic and splenic NKT cells isolated from B6 mice at different time points following injection of 4,000 sporozoites is shown. Cells were treated in vitro with phorbol myristate acetate, brefeldin, and ionomycin prior to surface and cytokine stainings. Numbers of cytokine-producing cells were determined by flow cytometry analysis of (A) hepatic $CD4^+$ NKT cells, (B) hepatic DN NKT cells, and (C) splenic $CD4^+$ NKT cells (gates were done as described in the legend of Fig. 1A). Data are representative of two independent experiments performed with three mice per time point. Results are expressed as mean values ± SD.

A.

| | | mean numbers of schizonts (SD) | % of inhibition |
|---|---|---|---|
| target cells: B6 hepatocytes | control wells | 315 (21) | 0 |
| | ratio 2.5/1 | 257 (20) | 18 |
| | ratio 5/1 | 215 (28) | 32 |
| target cells: B6.CD1d-/- hepatocytes | control wells | 106 (26) | 0 |
| | ratio 2.5/1 | 114 (23) | 0 |
| | ratio 5/1 | 120 (11) | 0 |

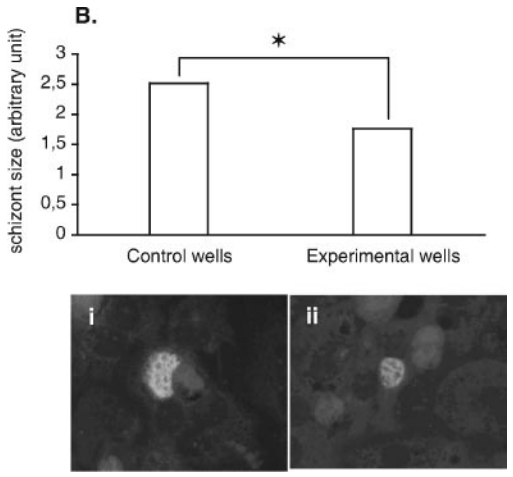


FIG. 7. In vitro inhibition assay of *P. yoelii* liver-stage development by parasite-activated hepatic DN NKT cells. (A) Sorted hepatic DN NK1.1$^+$ CD5$^+$ cells isolated from infected B6 mice at day 10 p.i. were added to primary cultures of B6 or B6.CD1d$^{-/-}$ hepatocytes at two different NKT cell/hepatocyte ratios (2.5/1 and 5/1) 3 h after sporozoite addition. Forty-five hours later, schizonts were quantified in control (only medium added) and experimental (DN NKT cells added) wells, and the mean of duplicate wells was calculated. Data representative of two independent and three independent experiments performed with B6 and B6.CD1d$^{-/-}$ hepatocytes, respectively, are shown. (B) Mean diameters ± SD of the intrahepatic schizonts in control and experimental wells of B6 hepatocyte cultures. *, the *P* value of <0.001. Representative pictures show schizonts found in control (i) and experimental (ii) wells (magnification, ×400).

lation increase during the infection but that a Th1-type cytokine response dominates. In addition, it is interesting to note that the DN subset displays a bias towards the production of IFN-γ and TNF-α compared to CD4$^+$ NKT cells. CD4$^+$ NKT cells isolated from infected spleens produced exclusively IFN-γ and TNF-α in response to stimulation, which differentiates them from the hepatic population of CD4$^+$ NKT cells found in infected livers.

**CD1d-dependent antiparasitic activity of *P. yoelii*-activated DN NKT cells in vitro against the hepatic stage.** We previously showed that *P. yoelii*-activated hepatic NKT cells inhibit the development of the parasite within hepatocytes in vitro, and DN NKT cells were suggested to be the main actors in this inhibition (34). Thus, we tested the capacity of hepatic DN NKT cells to inhibit the intrahepatic development of *P. yoelii* in vitro. We found that the number of intrahepatic schizonts decreased when *P. yoelii*-activated DN NKT cells were added to cultures (Fig. 7A). Moreover, this decrease in number was accompanied by a reduction in the size of the remaining parasites (Fig. 7B). Thus, *P. yoelii*-activated DN NKT cells can inhibit the maturation of the intrahepatic stage of the parasite in vitro.

As we observed that CD1d-dependent and -independent DN NKT cells were activated during the infection and that CD1d is constitutively expressed by murine hepatocytes (unpublished observation) (48), we addressed whether the antiparasitic activity of DN NKT cells was dependent on CD1d molecules. For that purpose, we added sorted hepatic DN NK1.1$^+$ CD5$^+$ cells, isolated from infected B6 mice at day 10, to sporozoite-infected B6.CD1d$^{-/-}$ hepatocyte cultures. As shown in Fig. 7A, under these conditions, the number of schizonts did not decrease, and we observed no effect on parasite size (data not shown). It is important to note that *P. yoelii* develops as efficiently in B6 and B6.CD1d-deficient hepatocytes (the differences in schizont numbers observed between control wells for these two strains of mice reflect differences in the infection efficiency, which is variable from one experiment to one another) (data not shown).

These results show that *P. yoelii*-activated DN NKT cells have the capacity to inhibit the intrahepatic stage of the parasite in vitro in a CD1d-dependent manner.

**CD1d and CD1d-dependent NKT cells are not required for the control of a primary *P. yoelii* infection in vivo.** Finally, we addressed the contribution of the CD1d-dependent NKT cell response to the control of the growth of *P. yoelii* in vivo. To evaluate the impact of the CD1d-dependent NKT cell response on the control of the preerythrocytic stage in vivo, we determined the parasite burden in the livers of B6 mice and B6.CD1d-deficient mice 44 h after infection by quantifying *P. yoelii* DNA. The results presented in Fig. 8A show that B6.CD1d-deficient mice and B6 control mice harbor the same quantities of parasites in their livers at this time point. Next, to determine whether the CD1d-dependent NKT cell response helps to limit erythrocytic development, we monitored the parasitemias of these two strains of mice starting 3 days after injection of sporozoites. We found no significant difference between the parasitemias of B6 and B6.CD1d-deficient mice (Fig. 8B).

Thus, we observed that B6.CD1d-deficient mice eliminate hepatic parasites and blood-stage parasites as efficiently as wild-type B6 mice. These results show that during primary infection induced by the injection of sporozoites, CD1d-dependent NKT cells play only a minor role in the control of the parasite's development in vivo.

## DISCUSSION

Our results show that the NKT cell response induced during a primary *P. yoelii* 265BY infection initiated by the injection of sporozoites is heterogeneous and differs between liver and

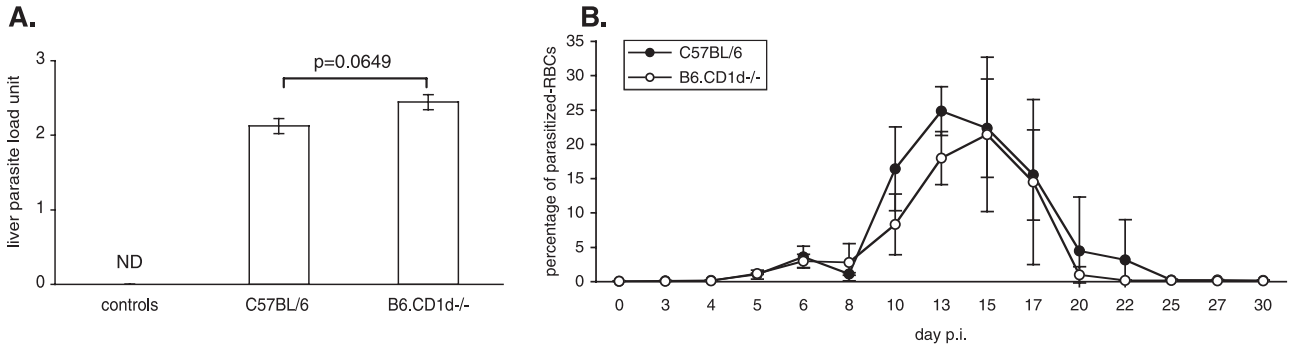


FIG. 8. Comparison of *P. yoelii* development in C57BL/6 and B6.CD1d$^{-/-}$ mice during primary infection. (A) Quantification of the parasite burden in the livers of noninfected (controls) (ND, not detected) and infected (44 h postinjection of sporozoites) B6 and B6.CD1d$^{-/-}$ mice. Results (means ± SD) from one representative experiment out of two performed with at least five mice per group are shown. The results are expressed in liver parasite load units, which correspond to the log numbers of parasite nuclei/0.5 μg of liver DNA. The difference between B6 and B6.CD1d$^{-/-}$ infected mice was close to significance ($P = 0.0649$). (B) Comparison of parasitemia in B6 ($n = 5$) and B6.CD1d$^{-/-}$ ($n = 4$) mice following infection with 4,000 sporozoites. Data are representative of two independent experiments, and results are expressed as mean values ± SD.

spleen, as shown by the marked phenotypic differences of hepatic and splenic NKT cells elicited during infection.

More precisely, NKT cells, which expand in the livers of infected B6 mice, consist of phenotypically and functionally distinct CD4$^+$ and DN subpopulations. CD1d-dependent CD4$^+$ NKT cells remained the largest NKT cell subpopulation in the livers of infected mice. These cells were mainly type I NKT cells expressing the invariant TCRVα14-Jα18 chain, as revealed by α-Galcer–CD1d tetramer staining and confirmed by the expression of the TCRVβ8.1/8.2 and Vβ7 segments (data not shown). Conversely, the expanded hepatic DN NKT cells were composed of an equal proportion of CD1d-dependent and -independent cells. Indeed, half of the DN NKT cells expressed the TCRVβ8.1/2 and TCRVβ7 chains (data not shown) and thus are expected to belong to the CD1d-dependent subpopulation of DN NKT cells, among which we found that the frequencies of type I and type II NKT cells were 60% and 40%, respectively. The other half of expanded hepatic DN NKT cells were CD1d-independent NKT-like cells. These cells may have arisen from conventional T cells upregulating the NK1.1 marker after activation, as has been shown during viral infection (45).

The increase in the numbers of hepatic NKT cell subsets correlates with cell activation, as shown by the up-regulation of the CD69 surface marker on CD4$^+$ and DN NKT cells. In addition, the proportion of CD62L$^+$ cells among DN NKT cells increased during infection. They represented more than 50% of the DN NKT cell subset on day 10 p.i. CD62L$^+$ DN NKT cells in naive mice have already been described and were shown to be CD1d-independent NKT cells expressing a diverse TCRαβ repertoire (8). These CD62L$^+$ DN cells may thus be NKT-like cells, as defined previously by Godfrey et al. (11). It is still unclear whether they play a particular role in the liver during *Plasmodium* infection. It is possible that CD62L$^+$ NKT cells from the spleen or the bone marrow are recruited to the liver during the course of infection, because these populations of NKT cells are preferentially found within these two organs in naive mice (8). Interestingly, we never observed an increase in CD62L$^+$ CD4$^+$ NKT cells in the liver at the same time points. Thus, the DN and CD4$^+$ subpopulations of hepatic NKT cells exhibit different characteristics and may play different roles during the immune response to *P. yoelii*.

On the contrary to what we observed for hepatic NKT cells, the majority of NKT cells isolated from the spleens of infected mice were CD4$^+$, CD1d independent, and noninvariant and presented no bias in the expression of the Vβ8.1/Vβ8.2 and Vβ7 chains of the TCR (data not shown). They thus display the phenotypic characteristics of type III NKT cells. The appearance of splenic CD4$^+$ and CD8$^+$ T cells expressing the DX5, ASGM-1, and NK1.1 markers during lymphocytic choriomeningitis virus infection in B6 mice has been reported (45). These cells, which accounted for more than 90% of the cells recognizing viral antigens, persisted for more than 500 days after infection and constituted a pool of memory cells. They also produced IFN-γ in vitro in the presence of viral antigens presented by classical class I and class II major histocompatibility complex molecules (45). Besides, memory CD8$^+$ T cells expressing the inhibitory receptor NKG2A but not Ly49 receptors appear during viral and bacterial infections (29), and it has been suggested that the expression of these receptors may modulate the activation signal transmitted by the TCR. Overall, these results are consistent with the hypothesis that the CD4$^{high}$ NKT cells that we found in the spleens of *P. yoelii*-infected mice are conventional T lymphocytes activated during the first week of infection and that these cells express the NK1.1 molecule following their activation. The persistence of these cells in the spleens of infected mice for 30 to 40 days after infection (our unpublished observations) also suggests that, as in viral infections, these cells may constitute a pool of memory cells. However, further investigations are required before firm conclusions can be drawn concerning the nature of the CD4$^{high}$ NKT cells appearing in the spleens of B6 mice during infection. Interestingly, we have never detected any population of T cells presenting such a phenotype in the liver during infection, at least up to day 10 p.i.

In addition, this population of splenic NKT cells induced during the infection displayed a peculiar TCRβ$^{high}$ CD4$^{high}$ phenotype, which may be the result of recent antigenic activation. Indeed, it has been reported previously that CD4$^+$ T cells restimulated in vitro or in vivo with their antigen increase the

number of TCRs and coreceptors expressed on their surface (9, 36).

We also found that the proportion of NKT cells expressing the inhibitory Ly49-A, -C/I, and -G2 receptors increased in the livers of infected mice, whereas they disappeared from the spleen during the infection. These observations reinforce the idea that the NKT cell response induced by *P. yoelii* is tissue specific. These inhibitory receptors expressed by hepatic NKT cells could be involved in the regulation of their activation within the liver. Indeed, Ly49 inhibitory receptors expressed by T cells and NKT cells have been proposed to dampen the effect of cell activation (32, 33, 44). We also confirmed that the activatory Ly49D receptor is not expressed on NKT cells in naive mice (42, 50) and showed that these cells do not start to express this receptor under inflammatory conditions resulting from infection. It is important to note that in most of our experiments, NKT cells were selected on the basis of the coexpression of the NK1.1 molecule and the TCRβ or the CD3 ε chains. Thus, it is possible that we failed to detect some NKT cells in which NK1.1 expression was down-regulated following activation (52).

NKT cells have the capacity to produce large amounts of Th1 and Th2 cytokines following stimulation, and splenic NKT cells were shown to secrete IFN-γ in response to infection with *P. berghei* ANKA-parasitized RBCs (16). Here, we observed that *P. yoelii*-activated hepatic and splenic NKT cells are both biased towards the production of IFN-γ and TNF-α, and not IL-4, following short-term in vitro stimulation. Interestingly, in the liver, the patterns of cytokines produced by the $CD4^+$ and DN subsets were different. Hepatic DN NKT cells were strongly biased towards the production of IFN-γ and TNF-α compared to $CD4^+$ NKT cells, which produced IFN-γ, TNF-α, and IL-4. To date, no particular bias towards the production of Th1- or Th2-type cytokines has been shown for the different subsets of murine NKT cells. On the contrary, in humans, $CD4^+$ and $CD4^-$ CD1d-dependent NKT cells have been defined as different functional subsets, with the latter exclusively producing Th1-type cytokines (14, 24). Thus, our results suggest that the same functional dichotomy may also exist for murine NKT cells under inflammatory conditions.

IFN-γ produced by splenic $CD4^+$ T cells has been shown to be necessary for establishing the appropriate immunoglobulin G response required to eliminate *P. chabaudi* blood-stage parasites (22, 23). Further investigations are required to determine whether the peculiar population of splenic NKT cells also helps to control the parasitemia and contributes to the protective immunity in our model.

As both CD1d-dependent and -independent hepatic and splenic NKT cells were expanded and activated during infection, we analyzed whether these two subsets of cells are involved in the control of *Plasmodium* development. We previously showed that total hepatic NKT cells, isolated from sporozoite-infected mice on day 10 p.i., exhibited parasitocidal activity against the liver stage in vitro. The DN subset of NKT cells was proposed to play a major role in this inhibition (34). Indeed, we show here that sorted *P. yoelii*-activated hepatic DN NKT cells inhibit the intrahepatic growth of the parasite in vitro. Moreover, we show that the in vitro inhibition of liver-stage development by DN NKT cells requires the expression of CD1d on the hepatocytes, as demonstrated by the absence of inhibition of parasite growth when B6.$CD1d^{-/-}$ hepatocytes were used. This observation raises numerous questions about the nature of the signal that activates these NKT cells and their subsequent inhibitory activity on the liver stage of *P. yoelii* in vitro. At least two different hypotheses can be proposed to explain these results. First, CD1d could present *Plasmodium*-derived antigens located on the surface of infected hepatocytes to the DN NKT cells, leading to their activation. Indeed, CD1d can present both exogenous and endogenous antigens to NKT cells (20, 27). Glycophosphatidylinositols from *Plasmodium falciparum* have been proposed to associate with CD1d and to activate NKT cells (41), but these results are controversial (30). Lipophosphoglycans from another protozoan parasite, *Leishmania donovani*, were shown to induce a Th1-polarized NKT cell response through a CD1d-dependent mechanism (1). Hence, it is conceivable that infected hepatocytes express CD1d molecules associated with parasite-derived antigens on their surface and that these complexes are recognized by DN NKT cells, leading to the elimination of the infected cells in vitro. As DN NKT cells were isolated from infected mice on day 10 p.i., this mechanism would imply that these cells recognize specific antigens expressed during the preerythrocytic stage only or antigens that are shared by both the preerythrocytic and erythrocytic stages of *Plasmodium* development. The second hypothesis is that CD1d, on noninfected as well as infected hepatocytes, could associate with an endogenous ligand. The recognition of such a self-antigen presented by CD1d, in the context of a proinflammatory cytokine environment, would lead to DN NKT cell activation. Indeed, Brigl and Brenner previously showed that the recognition of self-antigens presented by CD1d in the presence of IL-12 leads to IFN-γ production by invariant NKT cells during microbial infection (3). As DN NKT cells were isolated from infected mice at day 10 p.i. and were thus activated cells, they may not have needed additional proinflammatory stimuli to exert their parasitocidal effects in our in vitro assay.

Th1-type cytokines are required to establish a protective immune response to *Plasmodium* (7). In addition, IFN-γ secreted by invariant NKT cells following the injection of α-Galcer, their specific but artificial ligand, improves the efficiency of the protective T-cell response to *P. yoelii* 17X NL (13). Our results demonstrate that *P. yoelii*-activated NKT cells are biased towards the production of IFN-γ during the first week of a primary infection initiated by sporozoite injection. In our model of nonlethal malaria infection, this could favor the establishment of the protective immune response and improve its efficiency. However, our in vivo data show that the parasite load in the liver and the parasitemia of B6.$CD1d^{-/-}$ mice were not statistically different from those of B6 mice. This shows that despite their expansion and activation, CD1d-dependent NKT cells play only a minor role in the control of *P. yoelii* development during a primary infection in vivo. These results are partly consistent with those reported previously by Gonzalez-Aseguinolaza et al. (12), showing that α-Galcer-induced activation of CD1d-restricted NKT cells has no effect on the blood stage. However, in that same article, those authors showed that α-Galcer-activated NKT cells have a specific inhibitory effect on *P. yoelii* and *P. berghei* preerythrocytic development in vivo. Such discrepancies could be explained by the fact that in these latter experiments, NKT cells were activated

with their strong agonist, which is far from the physiological stimulation induced during plasmodial infection as in our system. Another explanation could be that in our model, other populations compensate for the absence of CD1d-dependent NKT cells because of a functional redundancy between different cell types. In support of this latter hypothesis, we and others showed that NK cells, γδT cells, and dendritic cells participate in the early immune response to *Plasmodium* (38, 49). Thus, these cells could be activated independently of CD1d-dependent NKT cells and be sufficient to control parasite development in vivo. In support of this idea, we observed that a primary infection of B6 mice with *P. yoelii* sporozoites induces the simultaneous activation of several populations of innate lymphocytes to produce IFN-γ early after infection (V. Soulard, unpublished data).

It is interesting to note that our in vitro results suggest that *P. yoelii*-activated CD1d-dependent NKT cells could exert an antiparasitic activity during their second encounter with infected cells, but further investigations would be required to address this question. However, for *Plasmodium* species that infect humans, the liver phase of parasite development lasts longer (6 to 14 days instead of 45 h in the case of *P. yoelii*). Since NKT cells reached a substantial level of activation and expansion in 4 to 6 days, they would be able to inhibit human malaria parasites that are still developing in the liver. Thus, the contribution of CD1d-dependent NKT cells to the control of the preerythrocytic stage of *Plasmodium* might be more important during human or primate malaria.

In conclusion, our work is one of the few to study the behavior and function of NKT cells in malaria during a primary *Plasmodium* infection initiated by the injection of the natural invasive form of the parasite. We show that the NKT cell response induced during a primary infection by *P. yoelii* presents the same characteristics of phenotypical heterogeneity as well as organ specificity compared to NK cells (38) and is mainly Th1 biased. It is interesting to note that this study reveals the involvement of CD1d-independent NKT cell subsets in the immune response induced during *Plasmodium* infection, and further investigations will be required to address the role played by these cells, for instance, whether they are involved in protection against secondary infection with *Plasmodium* sporozoites or in immune regulation.

## ACKNOWLEDGMENTS

This work was partly supported by the Programme de Recherche Fondamentale en Microbiologie, Maladies Infectieuses et Parasitaires (PRFMMIP) AO 2000, of the French Ministry of Research. V.S. was a recipient of fellowships from the French Ministry of Education and Research, the Fondation pour la Recherche Médicale, and the Fonds Inkermann from the Fondation de France.

We thank Anne Louise from the Flow Cytometry Platform for her help with NKT cell sorting (Institut Pasteur, Paris, France), Elodie Belnoue and Fabio Costa for their initial help in quantifying *P. yoelii* DNA in the liver, Danielle Voegtle for laboratory-made mAbs, and Denise Mattei for providing the I72 protein necessary for the preparation of the anti-liver-stage immune serum. We also thank Paul Brey, Isabelle Thiery, and Catherine Bourgouin for their help with the production and infection of *Anopheles stephensi* mosquitoes (Institut Pasteur, Paris, France). We are grateful to Mitchell Kronenberg for authorizing the use of murine CD1d tetramers and to Albert Bendelac for the gift of B6.CD1d-deficient mice.

## REFERENCES

1. **Amprey, J. L., J. S. Im, S. J. Turco, H. W. Murray, P. A. Illarionov, G. S. Besra, S. A. Porcelli, and G. F. Spath.** 2004. A subset of liver NK T cells is activated during Leishmania donovani infection by CD1d-bound lipophosphoglycan. J. Exp. Med. **200:**895–904.
2. **Bendelac, A., M. N. Rivera, S. H. Park, and J. H. Roark.** 1997. Mouse CD1-specific NK1 T cells: development, specificity, and function. Annu. Rev. Immunol. **15:**535–562.
3. **Brigl, M., and M. B. Brenner.** 2004. CD1: antigen presentation and T cell function. Annu. Rev. Immunol. **22:**817–890.
4. **Bruna-Romero, O., J. C. Hafalla, G. Gonzalez-Aseguinolaza, G. Sano, M. Tsuji, and F. Zavala.** 2001. Detection of malaria liver-stages in mice infected through the bite of a single Anopheles mosquito using a highly sensitive real-time PCR. Int. J. Parasitol. **31:**1499–1502.
5. **Carnaud, C., D. Lee, O. Donnars, S. H. Park, A. Beavis, Y. Koezuka, and A. Bendelac.** 1999. Cutting edge: cross-talk between cells of the innate immune system: NKT cells rapidly activate NK cells. J. Immunol. **163:**4647–4650.
6. **Doolan, D. L., and N. Martinez-Alier.** 2006. Immune response to pre-erythrocytic stages of malaria parasites. Curr. Mol. Med. **6:**169–185.
7. **Druilhe, P., L. Rénia, and D. A. Fidock.** 1998. Immunity to liver stages, p. 513. *In* I. W. Sherman (ed.), Malaria: parasite biology, pathogenesis, and protection. ASM Press, Washington, DC.
8. **Eberl, G., R. Lees, S. T. Smiley, M. Taniguchi, M. J. Grusby, and H. R. MacDonald.** 1999. Tissue-specific segregation of CD1d-dependent and CD1d-independent NK T cells. J. Immunol. **162:**6410–6419.
9. **Fasso, M., N. Anandasabapathy, F. Crawford, J. Kappler, C. G. Fathman, and W. M. Ridgway.** 2000. T cell receptor (TCR)-mediated repertoire selection and loss of TCR vbeta diversity during the initiation of a CD4(+) T cell response in vivo. J. Exp. Med. **192:**1719–1730.
10. **Fischer, K., E. Scotet, M. Niemeyer, H. Koebernick, J. Zerrahn, S. Maillet, R. Hurwitz, M. Kursar, M. Bonneville, S. H. Kaufmann, and U. E. Schaible.** 2004. Mycobacterial phosphatidylinositol mannoside is a natural antigen for CD1d-restricted T cells. Proc. Natl. Acad. Sci. USA **101:**10685–10690. [Epub ahead of print.]
11. **Godfrey, D. I., H. R. MacDonald, M. Kronenberg, M. J. Smyth, and L. Van Kaer.** 2004. NKT cells: what's in a name? Nat. Rev. Immunol. **4:**231–237.
12. **Gonzalez-Aseguinolaza, G., C. de Oliveira, M. Tomaska, S. Hong, O. Bruna-Romero, T. Nakayama, M. Taniguchi, A. Bendelac, L. Van Kaer, Y. Koezuka, and M. Tsuji.** 2000. α-Galactosylceramide-activated Vα14 natural killer T cells mediate protection against murine malaria. Proc. Natl. Acad. Sci. USA **97:**8461–8466.
13. **Gonzalez-Aseguinolaza, G., L. Van Kaer, C. C. Bergmann, J. M. Wilson, J. Schmieg, M. Kronenberg, T. Nakayama, M. Taniguchi, Y. Koezuka, and M. Tsuji.** 2002. Natural killer T cell ligand alpha-galactosylceramide enhances protective immunity induced by malaria vaccines. J. Exp. Med. **195:**617–624.
14. **Gumperz, J. E., S. Miyake, T. Yamamura, and M. B. Brenner.** 2002. Functionally distinct subsets of CD1d-restricted natural killer T cells revealed by CD1d tetramer staining. J. Exp. Med. **195:**625–636.
15. **Hansen, D. S., and L. Schofield.** 2004. Regulation of immunity and pathogenesis in infectious diseases by CD1d-restricted NKT cells. Int. J. Parasitol. **34:**15–25.
16. **Hansen, D. S., M. A. Siomos, L. Buckingham, A. A. Scalzo, and L. Schofield.** 2003. Regulation of murine cerebral malaria pathogenesis by CD1d-restricted NKT cells and the natural killer complex. Immunity **18:**391–402.
17. **Hansen, D. S., M. A. Siomos, T. De Koning-Ward, L. Buckingham, B. S. Crabb, and L. Schofield.** 2003. CD1d-restricted NKT cells contribute to malarial splenomegaly and enhance parasite-specific antibody responses. Eur. J. Immunol. **33:**2588–2598.
18. **Hulier, E., P. Petour, G. Snounou, M. P. Nivez, F. Miltgen, D. Mazier, and L. Renia.** 1996. A method for the quantitative assessment of malaria parasite development in organs of the mammalian host. Mol. Biochem. Parasitol. **77:**127–135.
19. **Kawano, T., J. Cui, Y. Koezuka, I. Toura, Y. Kaneko, K. Motoki, H. Ueno, R. Nakagawa, H. Sato, E. Kondo, H. Koseki, and M. Taniguchi.** 1997. CD1d-restricted and TCR-mediated activation of valpha14 NKT cells by glycosylceramides. Science **278:**1626–1629.
20. **Kinjo, Y., D. Wu, G. Kim, G. W. Xing, M. A. Poles, D. D. Ho, M. Tsuji, K. Kawahara, C. H. Wong, and M. Kronenberg.** 2005. Recognition of bacterial glycosphingolipids by natural killer T cells. Nature **434:**520–525.
21. **Kronenberg, M., and L. Gapin.** 2002. The unconventional lifestyle of NKT cells. Nat. Rev. Immunol. **2:**557–568.
22. **Langhorne, J., S. J. Meding, K. Eichmann, and S. S. Gillard.** 1989. The response of CD4+ T cells to Plasmodium chabaudi chabaudi. Immunol. Rev. **112:**71–94.
23. **Langhorne, J., B. Simon-Haarhaus, and S. J. Meding.** 1990. The role of CD4+ T cells in the protective immune response to Plasmodium chabaudi in vivo. Immunol. Lett. **25:**101–107.
24. **Lee, P. T., K. Benlagha, L. Teyton, and A. Bendelac.** 2002. Distinct functional lineages of human V(alpha)24 natural killer T cells. J. Exp. Med. **195:**637–641.
25. **Maeda, M., S. Lohwasser, T. Yamamura, and F. Takei.** 2001. Regulation of

NKT cells by Ly49: analysis of primary NKT cells and generation of NKT cell line. J. Immunol. **167:**4180–4186.
26. **Marsh, K., and S. Kinyanjui.** 2006. Immune effector mechanisms in malaria. Parasite Immunol. **28:**51–60.
27. **Mattner, J., K. L. Debord, N. Ismail, R. D. Goff, C. Cantu III, D. Zhou, P. Saint-Mezard, V. Wang, Y. Gao, N. Yin, K. Hoebe, O. Schneewind, D. Walker, B. Beutler, L. Teyton, P. B. Savage, and A. Bendelac.** 2005. Exogenous and endogenous glycolipid antigens activate NKT cells during microbial infections. Nature **434:**525–529.
28. **Mazier, D., R. L. Beaudoin, S. Mellouk, P. Druilhe, B. Texier, J. Trosper, F. Miltgen, I. Landau, C. Paul, and O. Brandicourt.** 1985. Complete development of hepatic stages of Plasmodium falciparum in vitro. Science **227:**440–442.
29. **McMahon, C. W., A. J. Zajac, A. M. Jamieson, L. Corral, G. E. Hammer, R. Ahmed, and D. H. Raulet.** 2002. Viral and bacterial infections induce expression of multiple NK cell receptors in responding CD8(+) T cells. J. Immunol. **169:**1444–1452.
30. **Molano, A., S. H. Park, Y. H. Chiu, S. Nosseir, A. Bendelac, and M. Tsuji.** 2000. Cutting edge: the IgG response to the circumsporozoite protein is MHC class II-dependent and CD1d-independent: exploring the role of GPIs in NK T cell activation and antimalarial responses. J. Immunol. **164:**5005–5009.
31. **Morens, D. M., G. K. Folkers, and A. S. Fauci.** 2004. The challenge of emerging and re-emerging infectious diseases. Nature **430:**242–249.
32. **Oberg, L., M. Eriksson, L. Fahlen, and C. L. Sentman.** 2000. Expression of Ly49A on T cells alters the threshold for T cell responses. Eur. J. Immunol. **30:**2849–2856.
33. **Ortaldo, J. R., R. Winkler-Pickett, A. T. Mason, and L. H. Mason.** 1998. The Ly-49 family: regulation of cytotoxicity and cytokine production in murine CD3+ cells. J. Immunol. **160:**1158–1165.
34. **Pied, S., J. Roland, A. Louise, D. Voegtle, V. Soulard, D. Mazier, and P. A. Cazenave.** 2000. Liver CD4−CD8− NK1.1+ TCR alpha beta intermediate cells increase during experimental malaria infection and are able to exhibit inhibitory activity against the parasite liver stage in vitro. J. Immunol. **164:**1463–1469.
35. **Renia, L., D. Mattei, J. Goma, S. Pied, P. Dubois, F. Miltgen, A. Nussler, H. Matile, F. Menegaux, M. Gentilini, et al.** 1990. A malaria heat-shock-like determinant expressed on the infected hepatocyte surface is the target of antibody-dependent cell-mediated cytotoxic mechanisms by nonparenchymal liver cells. Eur. J. Immunol. **20:**1445–1449.
36. **Ridgway, W., M. Fasso, and C. G. Fathman.** 1998. Following antigen challenge, T cells up-regulate cell surface expression of CD4 in vitro and in vivo. J. Immunol. **161:**714–720.
37. **Roland, J., and P. A. Cazenave.** 1992. Ly-49 antigen defines an alpha beta TCR population in i-IEL with an extrathymic maturation. Int. Immunol. **4:**699–706.
38. **Roland, J., V. Soulard, C. Sellier, A. M. Drapier, J. P. Di Santo, P. A. Cazenave, and S. Pied.** 2006. NK cell responses to Plasmodium infection and control of intrahepatic parasite development. J. Immunol. **177:**1229–1239.
39. **Schmieg, J., G. Gonzalez-Aseguinolaza, and M. Tsuji.** 2003. The role of natural killer T cells and other T cell subsets against infection by the preerythrocytic stages of malaria parasites. Microbes Infect. **5:**499–506.
40. **Schofield, L., and G. E. Grau.** 2005. Immunological processes in malaria pathogenesis. Nat. Rev. Immunol. **5:**722–735.
41. **Schofield, L., M. J. McConville, D. Hansen, A. S. Campbell, B. Fraser-Reid, M. J. Grusby, and S. D. Tachado.** 1999. CD1d-restricted immunoglobulin G formation to GPI-anchored antigens mediated by NKT cells. Science **283:**225–229.
42. **Shimizu, I., Y. Tomita, Q. W. Zhang, T. Iwai, G. Matsuzaki, and H. Yasui.** 2001. Different expressions of Ly-49 receptors on mouse NK and NK T cells. Immunobiology **204:**466–476.
43. **Sidobre, S., and M. Kronenberg.** 2002. CD1 tetramers: a powerful tool for the analysis of glycolipid-reactive T cells. J. Immunol. Methods **268:**107–121.
44. **Skold, M., and S. Cardell.** 2000. Differential regulation of Ly49 expression on CD4+ and CD4−CD8− (double negative) NK1.1+ T cells. Eur. J. Immunol. **30:**2488–2496.
45. **Slifka, M. K., R. R. Pagarigan, and J. L. Whitton.** 2000. NK markers are expressed on a high percentage of virus-specific CD8+ and CD4+ T cells. J. Immunol. **164:**2009–2015.
46. **Stevenson, M. M., and E. M. Riley.** 2004. Innate immunity to malaria. Nat. Rev. Immunol. **4:**169–180.
47. **Stevenson, M. M., and B. C. Urban.** 2006. Antigen presentation and dendritic cell biology in malaria. Parasite Immunol. **28:**5–14.
48. **Trobonjaca, Z., F. Leithauser, P. Moller, R. Schirmbeck, and J. Reimann.** 2001. Activating immunity in the liver. I. Liver dendritic cells (but not hepatocytes) are potent activators of IFN-gamma release by liver NKT cells. J. Immunol. **167:**1413–1422.
49. **Urban, B. C., R. Ing, and M. M. Stevenson.** 2005. Early interactions between blood-stage plasmodium parasites and the immune system. Curr. Top. Microbiol. Immunol. **297:**25–70.
50. **Voyle, R. B., F. Beermann, R. K. Lees, J. Schumann, J. Zimmer, W. Held, and H. R. MacDonald.** 2003. Ligand-dependent inhibition of CD1d-restricted NKT cell development in mice transgenic for the activating receptor Ly49D. J. Exp. Med. **197:**919–925.
51. **Watanabe, H., K. Ohtsuka, M. Kimura, Y. Ikarashi, K. Ohmori, A. Kusumi, T. Ohteki, S. Seki, and T. Abo.** 1992. Details of an isolation method for hepatic lymphocytes in mice. J. Immunol. Methods **146:**145–154.
52. **Wilson, M. T., C. Johansson, D. Olivares-Villagomez, A. K. Singh, A. K. Stanic, C. R. Wang, S. Joyce, M. J. Wick, and L. Van Kaer.** 2003. The response of natural killer T cells to glycolipid antigens is characterized by surface receptor down-modulation and expansion. Proc. Natl. Acad. Sci. USA **100:**10913–10918. [Epub ahead of print.]
53. **Zhou, D., J. Mattner, C. Cantu III, N. Schrantz, N. Yin, Y. Gao, Y. Sagiv, K. Hudspeth, Y. P. Wu, T. Yamashita, S. Teneberg, D. Wang, R. L. Proia, S. B. Levery, P. B. Savage, L. Teyton, and A. Bendelac.** 2004. Lysosomal glycosphingolipid recognition by NKT cells. Science **306:**1786–1789.

*Editor:* W. A. Petri, Jr.